JOURNAL OF GEOPHYSICAL RESEARCH, VOL. 103, NO. C3, PAGES 5477–5492, MARCH 15, 1998

Fifteen years of global wave hindcasts using winds from the European Centre for Medium-Range Weather Forecasts reanalysis: Validating the reanalyzed winds and assessing the wave climate

A. Sterl and G.J. Komen

Royal Netherlands Meteorological Institute, De Bilt

P.D. Cotton

James Rennell Division, Southampton Oceanography Centre, Southampton, England

Abstract. The ERA (European Centre for Medium-Range Weather Forecasts Reanalysis) project resulted in a homogeneous data set describing the atmosphere over a time span of 15 years, from 1979 to 1993. To validate (part of) these data against independent observations we use the ERA surface winds to drive the WAM wave model. The modeled significant wave heights are then compared with observations. From this comparison the quality of the forcing winds is assessed. The patterns of computed wave heights agree well with observed patterns, and they are of the right magnitude. This confirms the realistic nature of the ERA winds. If one looks in detail, it appears that the significant wave heights resulting from the model are systematically lower than the observed ones in areas of high winds and waves and higher in areas of low winds and waves. It is argued that underestimation at high winds speeds is most likely a resolution effect, as wind and thus wave peaks are missed by finite resolution in space and time, while overestimation at low wind speeds most likely results from internal WAM errors. It is concluded that the monthly mean ERA winds are slightly (less than 5%) too low in areas of high winds, while from this study it is not possible to draw a decisive conclusion on the quality of ERA winds at low wind speeds. At the same time, the hindcast data form a 15-year climatology of global waves. This climatology is analyzed in terms of annual cycle and trends. The largest trends in significant wave height occur in the North Atlantic with an increase of more than 12 cm/yr in January, and south of Africa where the increasing trend exceeds 7 cm/yr in July. These trends, however, are only marginally significant. Furthermore, they exhibit a large month-to-month variability, so that on a seasonal basis the trends are significant only in small parts of the ocean. In conclusion, we are unable to confirm a significant change in wave height during the ERA period.

1. Introduction

The European Centre for Medium-Range Weather Forecasts (ECMWF) Reanalysis project (ERA) has recently been completed [*Gibson et al.,* 1996]. It produced a 15-year-long data set (January 1979 to February 1994) providing a detailed description of the atmosphere. Unlike the daily operational analyses that have been performed at ECMWF since 1979, this series is homogeneous as far as the analysis technique is concerned.

Paper number 97JC03431.
0148-0227/98/97JC-03431$09.00

Furthermore, much more data have been used for the reanalysis than were available operationally. While this is thought to be advantageous for the quality of the result, there are only few (if any) independent data left for validation.

To overcome part of this problem, one can consider using the ERA output to calculate quantities that have not been used in the reanalysis process and compare them with respective observations. For example, *Stockdale* [1996] uses the ERA surface fluxes of heat and momentum to drive an ocean general circulation model (GCM) to conclude on the quality of these fluxes.

Here we adopt this approach by using the ERA surface winds to drive the WAM wave model [*Komen et al.,* 1994]. Modeled wave heights are then compared with observations. As wave height observations are not used in the atmospheric analysis scheme, this is an independent test of the ERA surface winds. The problem with this approach is, however, that the model error of the wave model is introduced as an additional error source.

As a very interesting by-product of this procedure, a 15-year climatology of global wave characteristics is obtained. Although this climatology comprises a variety of quantities (see the appendix for a detailed description of data sets), the first assessment of this climatology given here is confined to significant wave height.

2. Tools

2.1. The ECMWF Reanalysis Project

The ERA project [*Gibson et al.,* 1996] has been one of the major undertakings of ECMWF during the last few years. All available meteorological data from the 15-year period January 1979 to February 1994 have been used to produce a homogeneous description of the atmosphere. At the heart of ERA was the ECMWF numerical weather prediction scheme with the assimilation scheme and the atmospheric general circulation model (AGCM) as its main constituents. ERA used a GCM version with a horizontal resolution of T106 and 31 levels in the vertical. Nominally, T106 corresponds to $\approx 1.2°$, but due to the horizontal diffusion that filters out the high-frequency part of the energy spectrum the effective resolution is only $\approx 2°$. The observational data were passed through the assimilation scheme and used to update the GCM every 6 hours. The 10-m winds (U_{10}) from that analysis are used in this study to drive the WAM model.

Due to problems discovered during the ERA production process, part of the ERA period had to be rerun, resulting in different experiment versions [*Gibson et al.,* 1996]. However, tests showed that the impact of these different winds on wave heights was small, generally not exceeding 10 cm on a monthly mean basis. Therefore, only results from the original ERA run, known as experiment version 1, are considered here.

2.2. The WAM Wave Model

2.2.1. Model description. The wave model used in this study is cycle 4 of the WAM model. The WAM model was developed by the Wave Modeling group [*WAMDI Group,* 1988]. Cycle 4 of the model is described by *Komen et al.* [1994], so only a very short description is given below. For reasons that will become apparent in section 3.1, the model has been used with two different resolutions. The low-resolution (LR) version has a 3° × 3° grid covering the whole globe between 72°N and 63°S, while the high-resolution (HR) version has a 1.5° × 1.5° grid covering the globe between 81°N and 81°S, taking sea ice into account. More details about the runs performed can be found in the appendix.

The state of the sea is usually described by the wave variance spectrum $F(\vec{k},\vec{x},t)$, where $\vec{k}$ denotes the wavenumber vector, $\vec{x}$ the position, and t time. The physical meaning of F is that the total wave energy per unit area is given by $\overline{E(\vec{x},t)} = \rho_w g \int d\vec{k}\, F(\vec{k},\vec{x},t)$, where ρ_w is the density of water and g the acceleration due to gravity. Another important quantity is the significant wave height, which can be calculated from F as

$$H_S(\vec{x},t) = 4\left[\int d\vec{k}\, F(\vec{k},\vec{x},t)\right]^{1/2} = 4\left[\frac{\overline{E(\vec{x},t)}}{\rho_w g}\right]^{1/2}. \tag{1}$$

In the deep water approximation, which is appropriate for a global run, the evolution of F is described by the energy balance equation

$$\frac{\mathrm{D}F}{\mathrm{D}t} = S_{in} + S_{nl} + S_{ds}, \tag{2}$$

where $\mathrm{D}/\mathrm{D}t$ denotes differentiation when moving with the group velocity. The three source terms on the right-hand side denote the input of energy by wind (S_{in}), nonlinear interaction between waves (S_{nl}), and dissipation by whitecapping (S_{ds}). The term relevant for our aim of validating the ERA winds is, of course, the wind input source term

$$S_{in} = f(\vec{\tau})\, F, \tag{3}$$

with f being a complicated function of wind stress $\vec{\tau}$. Note that S_{in} depends on the full spectrum F.

The wind stress $\vec{\tau}$ is related to the wind $\vec{U}$ by

$$\vec{\tau} = \rho_a C_D U \vec{U}, \tag{4}$$

where $U = |\vec{U}|$ and ρ_a is the density of air. The drag coefficient C_D depends on the reference height z_{obs} at which $\vec{U}$ is measured. Usually, $z_{obs} = 10\,\mathrm{m}$ is used, and this value will be used throughout this paper. Furthermore, the drag coefficient depends on the roughness length z_0, which in turn depends on the magnitude of the stress and the sea state,

$$C_D = [\kappa/\ln(z_{obs}/z_0)]^2, \tag{5}$$

$$z_0 = \frac{\hat{\alpha}\tau}{g\sqrt{1-\tau_w/\tau}}. \tag{6}$$

Here $\kappa = 0.4$ is the von Kármán constant, $\hat{\alpha}$ is a constant whose value has been found to be 0.01, and τ_w is the wave-induced stress or wind-to-waves momentum transfer, given by

$$\tau_w = \rho_w g \int d\vec{k}\, S_{in}/c, \tag{7}$$

where ρ_w is the density of water and c the phase speed. Through (3) τ_w depends on the full wave spectrum.

Using (4) to (7), the WAM model calculates the wind stress from $\vec{U}_{10}$ (here taken from ERA) and F (taken from the wave spectrum estimate obtained in the previous time step) and then solves the energy balance equation (2).

2.2.2. Model performance. The WAM model has been tested extensively, usually under high-wind conditions. For example, *Cardone et al.* [1995] showed that the model reproduces observed wave heights very well, provided that the model is driven by the correct winds. It turns out that the input wind is the crucial parameter for obtaining the right wave height. This also implies that the approach followed here, that is, assessing the quality of a wind data set by using it to drive a wave model, is a powerful tool. However, the calculations of *Cardone et al.* [1995] were done on a grid with 0.25° resolution, much finer than the grid used here.

Janssen et al. [1996] assessed the quality of ECWMF's Wave Forecasting System, the heart of which is formed by the same 1.5° version of WAM that is used here as the HR version. When comparing their analysis with buoy data, they found a typical wave height bias of $-0.25\,\mathrm{m}$ and a scatter index of 0.2 (see section 3.2 for definitions). In that analysis, wave observations from ERS 1 have been assimilated, which are known to have a negative bias. Comparing their first guess (i.e., a 6-hour forecast starting from an analyzed wave field) with altimeter wave heights, they found a bias of $+0.2\,\mathrm{m}$, while the scatter remained the same.

For fully developed sea an empirical relation between significant wave height and wind reads [*Sanders,* 1976; *Janssen et al.,* 1984]

$$H_S = \frac{\beta}{g}U_{10}^2 \Longleftrightarrow dH_s = 2\frac{\beta}{g}U_{10}dU_{10} = 2H_S\frac{dU_{10}}{U_{10}}, \quad (8)$$

where $\beta = 0.22$. Then, for typical values of $U_{10} = 10\,\mathrm{m/s}$ and $H_S = 4\,\mathrm{m}$, a wave height bias of $\pm 0.2\,\mathrm{m}$ corresponds to a wind bias of $\approx \pm 0.25\,\mathrm{m/s}$. The WAM model can thus be expected to assess the quality of the wind input to within this accuracy. However, the true biases may be higher, as these estimates use output from a model into which wave observations have been assimilated. Furthermore, in the real ocean, high waves are rarely, if ever, fully developed, and so the actual relationship between wind speed and wave height is much more complex.

2.3. Data Sources

To assess the quality of the modeled wave heights, two data sets are used for comparison. *Carter et al.* [1992] and *Cotton and Carter* [1994] calibrated the altimeter data from Geosat, ERS 1 and Topex/Poseidon against buoy data. The *Carter et al.* [1992] calibration resulted in an increase in the wave heights from the Geosat altimeter by 13%, and the *Cotton and Carter* [1994] calibration resulted in a recommendation to apply a linear correction to ERS 1 OPR (Ocean Product) data according to $H_S(\text{ERS-1}) = 0.824 - 0.107 \cdot H_S(\text{buoy})$. (In the original paper this equation appeared incorrectly, and a correction was published.) Monthly means of significant wave heights calculated from Geosat GDR (Geophysical Data Record) data for the period January 1987 to September 1989 and from ERS 1 OPR data for April 1992 to December 1993, adjusted according to the findings of the above papers, are used here. The data were averaged onto the same $3° \times 3°$ grid that is used in the LR version of WAM.

To assess not only monthly means but also the high-frequency properties of the model results, buoy measurements as compiled and distributed by the National Data Buoy Center (NDBC) of the National Oceanic and Atmospheric Administration (NOAA) (http://seaboard.ndbc.noaa.gov/) are used. In this paper, only a few examples are shown.

3. Verifying the Hindcast

3.1. Verification Against Altimeter Data

Figure 1 shows the mean significant wave height for January 1988 as obtained from the two model versions and from the altimeter, respectively. The patterns of modeled and observed wave heights are in close agreement. However, the modeled wave heights are too low, especially at higher latitudes. The difference between model and data exceeds 1 m at certain places for the LR version. Although the HR version also underestimates the altimeter-derived wave heights, it is obvious that for this version the deviations are much smaller and generally do not exceed 0.5 m. Therefore, further discussions in this paper will concentrate on the HR version.

Figure 2 displays the difference in H_S between HR model and altimeter for January and July 1988. Comparison with Figure 1 shows that the largest underestimation occurs in areas of large mean wave heights, especially in the western parts of the northern oceans. Areas of large mean wave height are also the areas of highest mean wind speeds (not shown). At the same time, the model overestimates H_S in areas of low waves and winds.

Figure 3 shows the difference $H_S(\text{HR mod}) - H_S(\text{alt})$, averaged over the two hemispheres as well as the tropics (between 15°N and 15°S), as a function of time (thick curves). As can be seen, the model-data misfit (bias) has a pronounced annual cycle in both hemispheres with underestimation in the winter hemisphere and overestimation in the summer hemisphere, while in the tropics, model results are higher than observations throughout the year. In the southern hemisphere (SH) the underestimation during winter is larger and the overestimation during summer lower than it is in the northern hemisphere (NH). This is in accord with the above observation of the model underestimating high and overestimating low waves: Waves are higher during winter than during summer and larger in the SH than in the NH and lowest in the tropics (see section 4.1 below). Furthermore, Figure 3 shows that Figures 1 and 2 are typical for the whole period (1987-1993). There is no evidence of either a trend in bias or any differences between the data from the two satellites involved.

Figure 3 compares data from the HR version of the model with altimeter data. For output from the LR version of the model (not shown), the corresponding

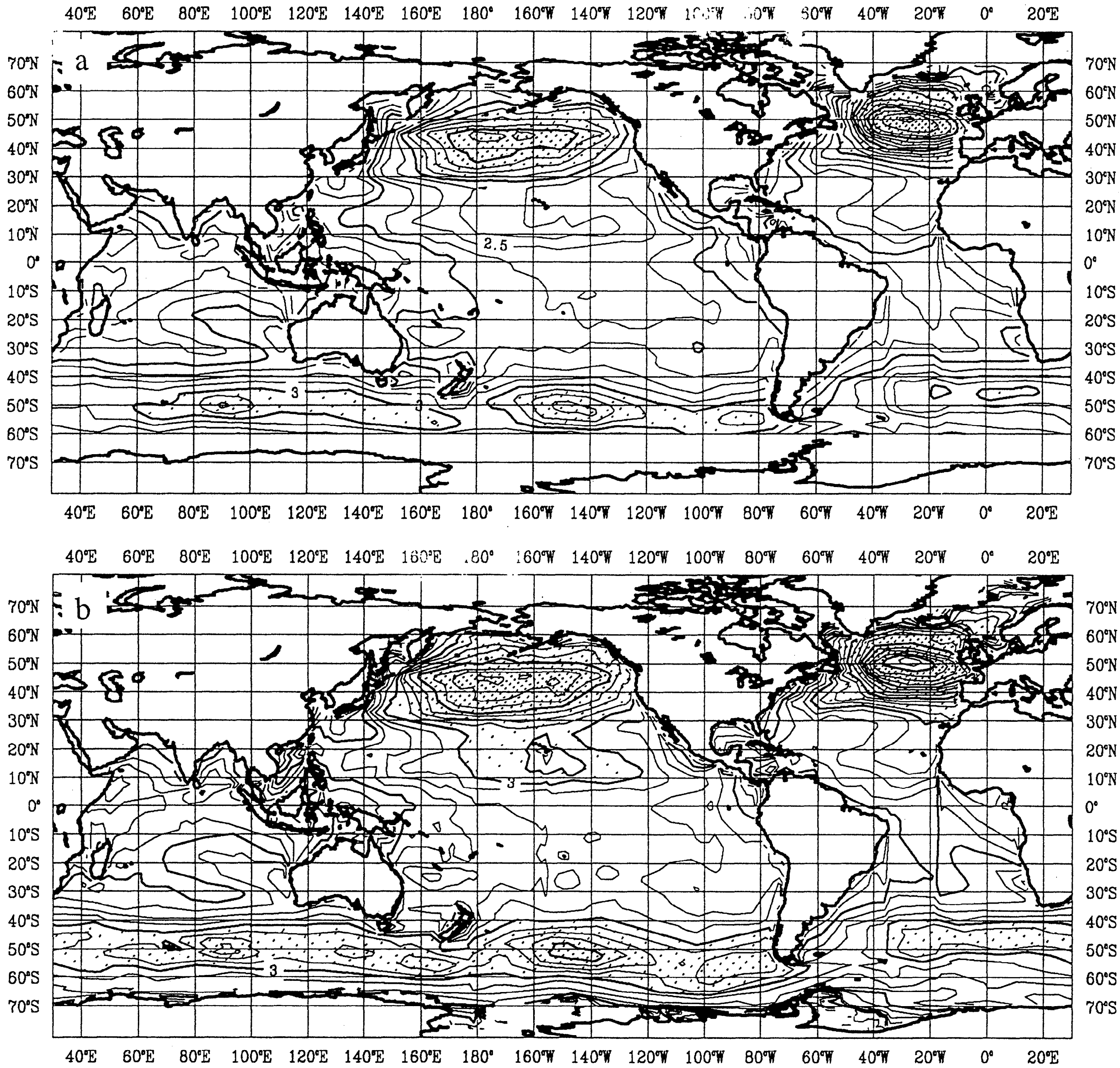

Figure 1. Monthly mean wave height for January 1988 from (a) the LR model, (b) the HR model, and (c) the altimeter measurements. Contour interval is 0.25 m with stippling between 3 m and 6 m. Every fourth line is thickened.

curves of area-averaged bias are simply shifted downward by 20 to 30 cm (i.e., they become more negative), so that even in the tropics H_S is slightly underestimated. *Romeiser* [1993] compared uncorrected Geosat altimeter data with data obtained from driving an earlier version of WAM with winds from the then operational ECMWF model. Both the AGCM and WAM had the same horizontal resolution as our LR version, that is, T106 and 3°, respectively. He found good agreement between the two data sets in the NH, while WAM underestimated the wave heights in the SH in winter by about 20% and overestimated low wave heights. The first problem was attributed to the input winds being too low.

At first sight, the results of *Romeiser* [1993] (for the NH) are apparently better than those from our LR version. However, as stated above, he used uncorrected altimeter data which have been shown to be too low [*Carter et al.,* 1992]. Furthermore, the operational ECMWF model used in 1988 contained an error resulting in the surface winds used to drive WAM systematically being too high [*Janssen et al.,* 1992]. Both effects work so as to bring modeled and observed wave heights closer together into apparently better agreement.

3.2. Verification Against Buoy Data

To investigate the performance of the model on shorter than monthly timescales, buoy data collected by

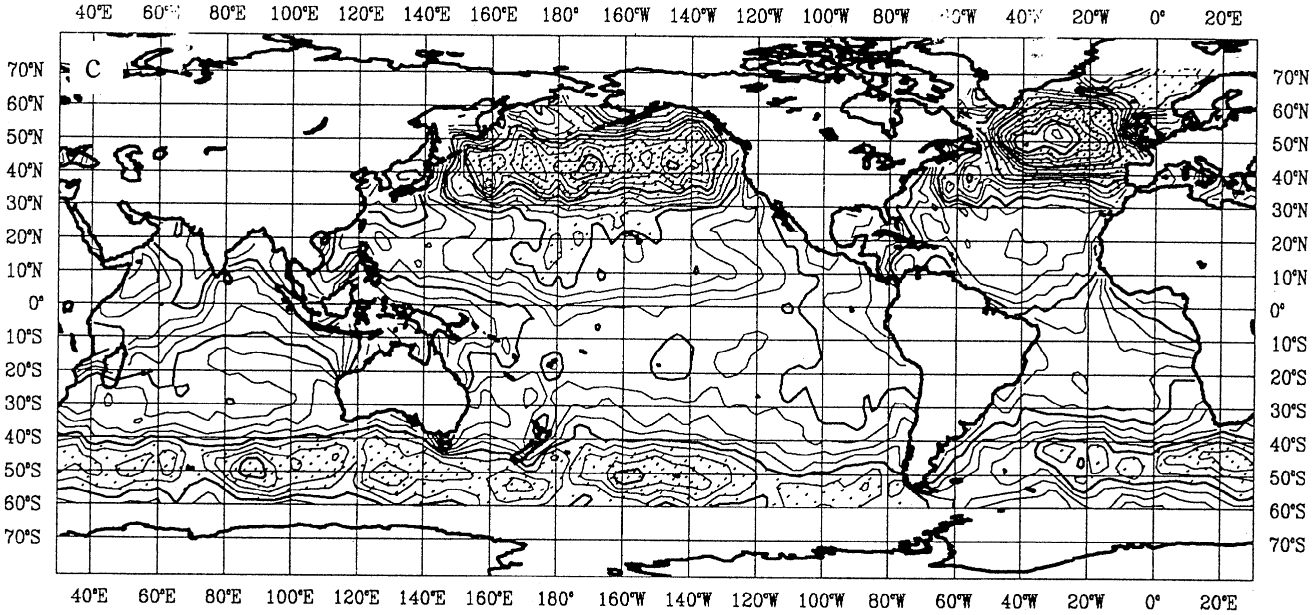

Figure 1. (continued)

NDBC have been selected and compared with the model results at the buoy's position. Buoy data have been extracted for different years and for two seasons (winter (JFM) and summer (JA)) according to the availability of a continuous time series. The raw buoy data are used: only obviously erroneous data (wind but no waves) have been removed. Table 1 lists the buoys used along with characteristics of the comparison with modeled data for both the LR and the HR version of the model.

To judge the quality of the simulation we use bias, scatter index, and unbiased regression slope. The bias is the mean of the error $x = H_S(\text{model}) - H_S(\text{buoy})$ and measures the mean deviation between buoy and model. The scatter index SI is the RMS error (standard deviation of x) normalized by the mean of the reference (buoy) and measures the confidence one can have in that deviation. The unbiased regression slope b is the result of a regression analysis in which neither of the two data sets (H_S(model) and H_S(buoy)) is regarded as perfect, but as contributing equally to the error. Ideally, $b = 1$. If $b > 1$, H_S(model) tends to overpredict high or underpredict low waves, while the opposite is true for $b < 1$.

From Table 1 the following observations can be made: (1) The bias is negative, that is, the model underestimates H_S, if H_S is large (winter, high latitudes). (2) At low H_S, the model overpredicts. (3) In accordance with the two foregoing observations, b is always less than 1. (4) The scatter index is higher for the Atlantic buoys than for those in the Pacific. (5) The Atlantic buoys have the largest (negative) bias. (6) There is no difference in SI between summer and winter, a typical value being 0.2 for the HR version, but b is closer to 1 in winter. (7) The buoy–model bias receives a positive increment when moving from the HR model to the LR model; thus an underestimation seen in the LR output becomes less or even changes to an overestimation in the HR data, while overestimation becomes larger. (8) Compared to the LR model, the HR model has a lower scatter index and a regression slope that is closer to 1. (9) The smallest values of b occur for two of the Hawaiian buoys.

Concerning the bias, these observations are in agreement with the comparisons with altimeter data in section 3.1, while the lower SI and higher regression slopes for the HR model suggest that the higher resolution not only results in higher, but also in "better" waves. As argued by *Komen et al.* [1994, pp. 306-307], the typical value of 0.2 for the scatter index is close to the expected minimum value at the given resolution. While this value has also been found by *Janssen et al.* [1996], they never find positive biases.

The low regression slopes for the two Hawaiian buoys 51003 and 51004 are the result of a storm badly captured by ERA. On July 23, 1986 these buoys registered wind speeds of more than 20 m/s and wave heights reaching 10 m. This storm is also present in ERA, but at a slightly different position and with smaller wind speeds. At the position of buoy 51003, ERA shows no signs of a storm at all. At the position of buoy 51004, ERA winds reach a maximum of 15.3 m/s, giving rise to a significant wave height of 3.9 m, while the buoy records a wind speed of 22.9 m/s and a wave height of 9.8 m. If we recalculate the regression slope leaving out data from July 23, the slope values (for HR) change to 0.55 for both buoys. These values are within the range of those for other buoys. That the storm is badly captured is probably due to ERA's limited resolution in space and time. This aspect will be discussed in more detail in sections 3.3.2 and 3.3.3.

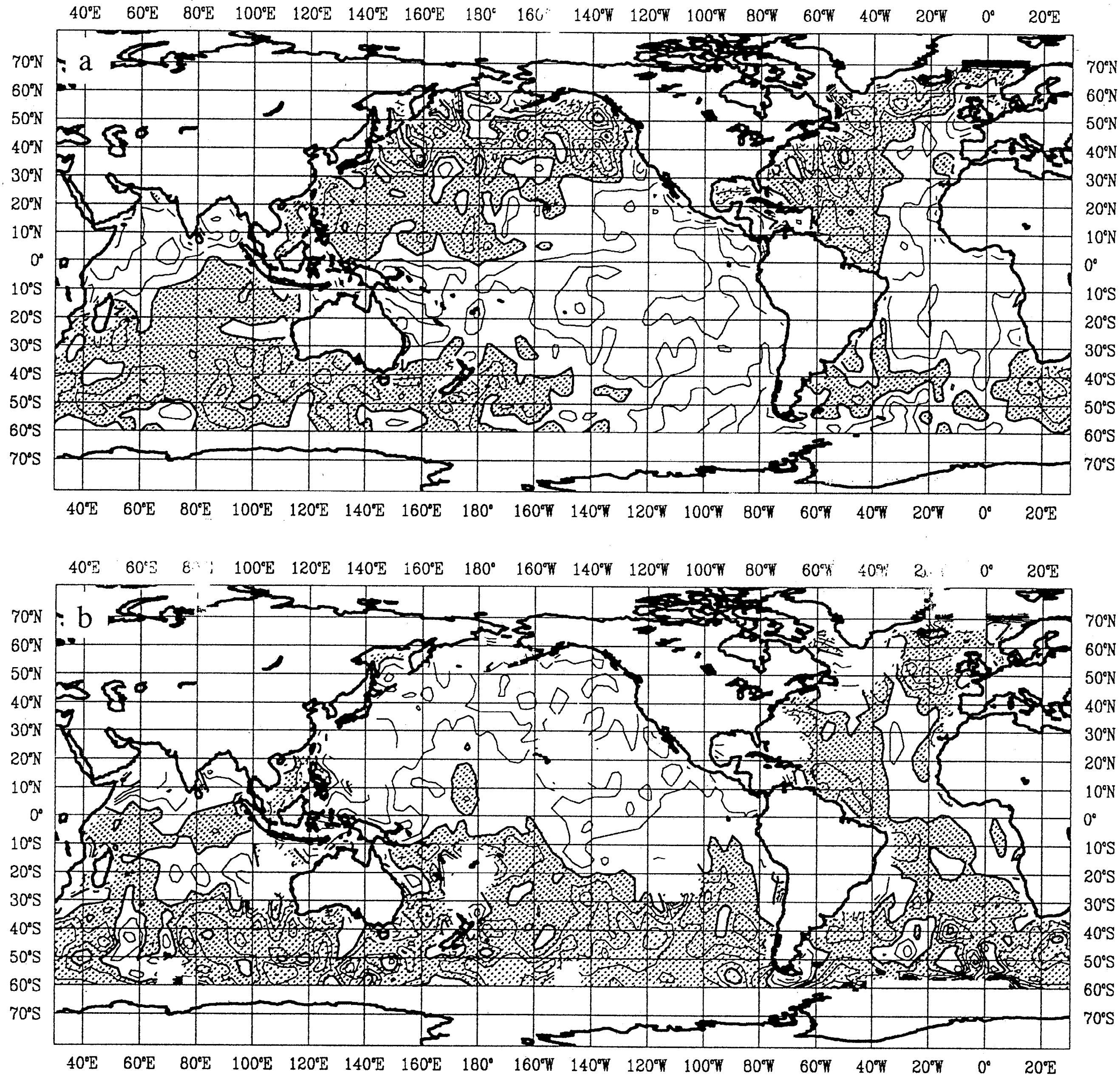

Figure 2. Difference of monthly mean wave height between HR model and altimeter measurement for (a) January and (b) July 1988. Contour interval is 0.25 m with negative values stippled.

Figure 4 gives a typical picture of how measured and modeled data are related. During winter (Figures 4a and 4b) modeled wave heights follow the measured ones very closely, but peaks are underestimated, giving rise to the underestimation of monthly mean wave heights noted above. During summer (Figures 4c and 4d), modeled variability is less than observed, but modeled H_S is nearly always higher than measured. This overestimation of low wave heights has also been noticed by *Romeiser* [1993].

In both seasons, wave heights from the HR version are higher than those from the LR version. However, during winter (generally high waves) these higher model waves suggest that the peaks in the buoy data are better represented, leading to the impression that the HR version is really an improvement compared to the LR model. In fact, it can be seen from Figures 4c and 4d that during summer (generally low waves) the higher HR waves are the result of a shift toward a higher background level. As the background level in the LR version is already too high, this increase represents an undesirable characteristic in the model. From Table 1 it may be inferred that these results are also typical for other buoys.

3.3. Discussion of Discrepancies Between Hindcast and Observations

The results from the comparisons of modeled with satellite-derived and buoy-measured data, respectively, are consistent and can be summarized as follows: (1)

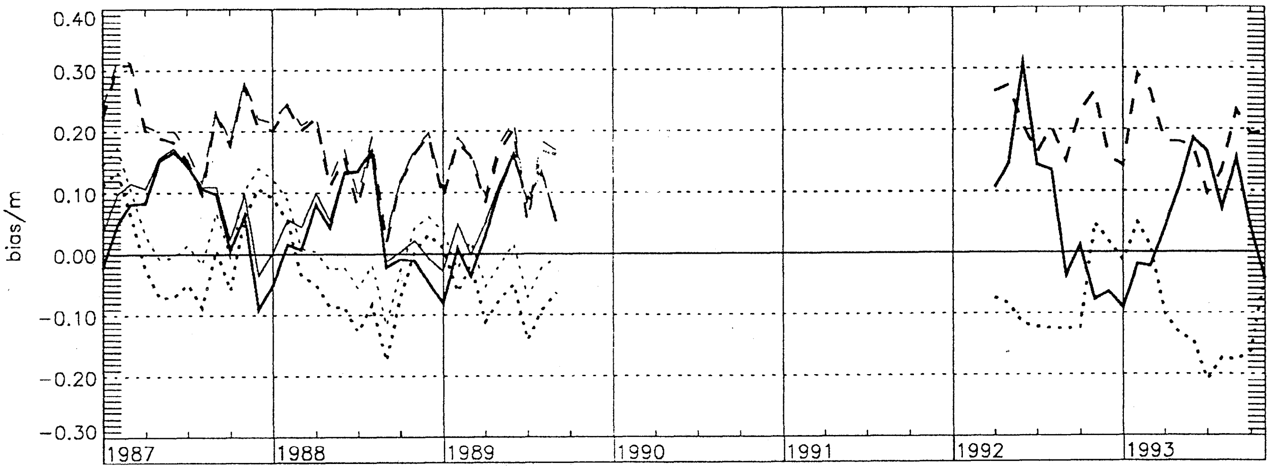

Figure 3. Difference of monthly mean wave height between HR model and altimeter measurement as a function of time (solid: NH, dotted: SH, dashed: tropics). The thin curves are for the corrected Geosat data; see section 3.3.1.

Table 1. Wave Statistics at Selected Buoys

			Winter (JFM)					Summer (JA)				
Buoy	Position	Year	N	H_S	Bias	SI	b	N	H_S	Bias	SI	b
					North Atlantic							
44011	41°06′N	1988	144	2.51	-0.56	0.27	0.67	120	1.32	-0.36	0.27	0.35
	66°36′W				-0.34	0.22	0.72			-0.13	0.25	0.45
44004	38°30′N	1986	176	2.54	-0.85	0.26	0.61	98	1.30	-0.39	0.43	0.33
	70°36′W				-0.42	0.22	0.73			-0.11	0.32	0.57
41002	32°12′N	1987	177	2.73	-0.88	0.27	0.56	122	1.20	-0.36	0.21	0.46
	75°18′W				-0.58	0.23	0.66			-0.14	0.19	0.61
					Gulf of Mexico							
42001	25°54′N	1987	173	1.53	-0.46	0.36	0.53	122	0.51	0.01	0.41	0.41
	89°42′W				-0.28	0.26	0.72			0.07	0.33	0.72
42003	26°00′N	1986	175	1.34	-0.34	0.36	0.53	122	0.66	-0.12	0.36	0.23
	85°54′W				-0.21	0.26	0.72			-0.10	0.26	0.50
					Hawaii							
51001	23°24′N	1986	120	3.02	-0.14	0.35	0.46	122	2.07	0.02	0.14	0.51
	162°18′W				0.21	0.20	0.74			0.32	0.15	0.70
51002	17°11′N	1986	176	2.57	0.01	0.19	0.65					
	157°48′W				0.36	0.19	0.90					
51003	19°12′N	1986	177	2.62	-0.01	0.16	0.66	122	2.04	0.07	0.18	0.23
	160°48′W			0.26	0.16	0.87			0.26	0.20	0.23	—
51004	17°30′N	1986	177	2.67	-0.04	0.17	0.63	120	2.26	-0.03	0.30	0.19
	152°36′W				0.06	0.15	0.62			0.22	0.29	0.24
					North Pacific							
46001	56°18′N	1988	179	3.76	-0.77	0.19	0.69	122	1.72	-0.09	0.29	0.46
	148°18′W				-0.21	0.19	0.78			0.21	0.25	0.57
46006	40°48′N	1987	173	3.96	-0.53	0.19	0.62	122	1.76	0.34	0.21	0.64
	137°36′W				-0.13	0.17	0.71			0.55	0.18	0.71
46035	57°00′N	1988	169	3.02	-0.17	0.21	0.81	112	1.47	0.19	0.25	0.57
	177°42′W				0.13	0.17	0.89			0.45	0.23	0.68
46036	48°18′N	1987	168	3.92	-0.81	0.19	0.54	120	1.70	0.18	0.19	0.67
	133°54′W				-0.32	0.17	0.68			0.38	0.20	0.65

H_S is mean significant wave height from buoy; N is the number of observations. The first row in the bias, SI (scatter index) and b (unbiased regression slope) entries refers to the LR version, the second to the HR version of WAM. Values for bias are in meters.

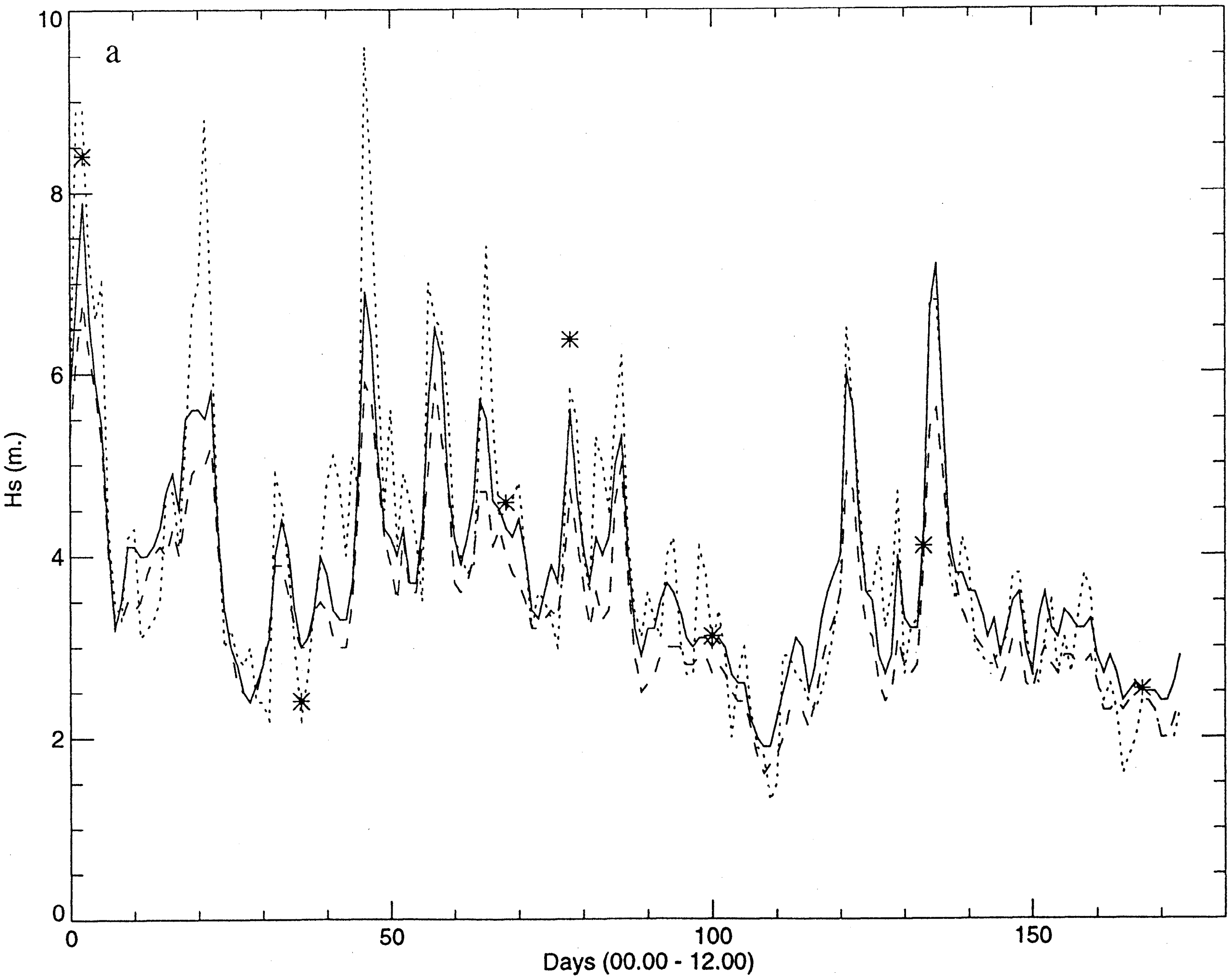

Figure 4. (a) Time series and (b) scatterplot of modeled and measured H_S for winter (January, February, March (JFM)) for buoy 46006 in 1987; (c) time series and (d) scatterplot of modeled and measured H_S for summer (July-August (JA)), with HR version only in Figure 4d. In Figures 4a and 4c the solid line is for WAM-HR, the dashed line is for WAM-LR, the dotted line is for the measurements, and the stars represent altimeter measurements at the buoy's position. The lines in Figures 4b and 4d are the unbiased regression lines.

At high H_S the model captures the measured variability well, but underestimates wave height; peaks are too low. (2) At low H_S the model underestimates the measured variability, but overestimates wave height.

Basically, there are four possible sources for the mismatch between modeled and measured wave heights, namely, (1) observation error, (2) insufficient model (WAM) resolution, (3) general model (WAM) error (apart from resolution), and (4) reanalysis error. These four possible reasons will now be discussed separately.

3.3.1. Observation error. The Geosat altimeter data as used in this study are the original data increased by a factor of 1.13 according to *Carter et al.* [1992]. In more recent work on the intercalibration of buoy and altimeter data, P.D. Cotton and D.J.T. Carter (Calibration and validation of ERS 2 altimeter wind/wave measurements, Southampton Oceanography Centre, Internal Document 12, 119 pp. unpublished manuscript (D.R.A. I.T.T CSM/078), 1996) revisited the Geosat data, using for consistency with their other analyses a principal components regression rather than a simple one-way regression. This work indicated that a smaller correction of only 6.5% should be applied to the Geosat data. Figure 3 (thin curves) shows that this recalibration does not lead to an improvement. Furthermore, both the ERS 1 data (1992/1993) and the comparison with buoy measurements (section 3.2) are unaffected. Therefore we conclude that errors in the altimeter measurements cannot explain the discrepancies.

The altimeter measurements are calibrated by comparison with buoys. So errors in the buoy measurements could spoil the altimeter data used to compare

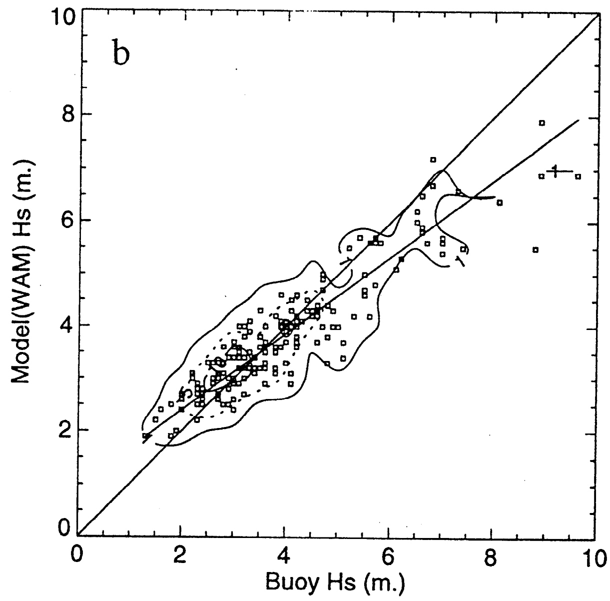

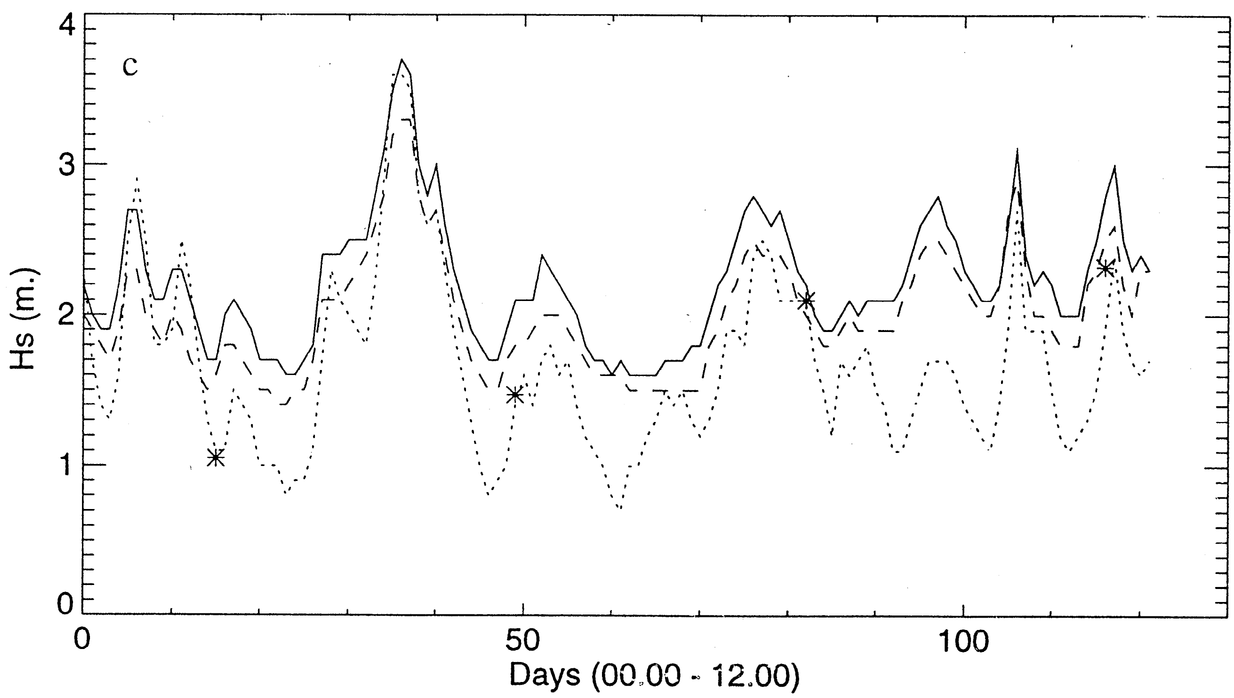

Figure 4. (continued)

the modeled data with. Explaining the discrepencies found in this manner would require buoys to systematically overestimate high and underestimate low waves. To our knowledge there is no evidence indicating that this is the case.

3.3.2. Model resolution. The improvement of the HR model compared to the LR model may have two sources, namely, (1) the higher resolution of the wave model, and (2) the higher resolution of the input wind. An integration with the WAM model at high resolution, but winds interpolated from the low-resolution grid, gave results nearly identical to that from the LR model (not shown). This indicates that the limiting factor is the quality of the wind rather than the resolution of the model, confirming results of, for example, *Zambresky* [1989], who found that increasing the resolution of the wave model only affects the results if that higher resolution also provides a better representation of the wind field, that is, a better representation of gradients in the wind field, or *Graber et al.* [1995], who artificially reduced the resolution of the input wind, but kept the resolution of the wave model.

The comparison between the results from the LR and the HR versions of WAM showed that increasing the resolution has a beneficial effect in situations of high and highly variable H_S, while at low wave heights the

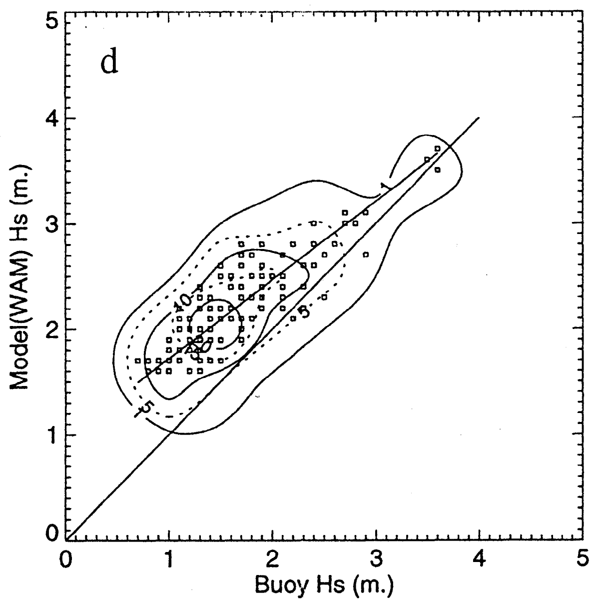

Figure 4. (continued)

model results became worse at higher resolution. According to the above discussion, the improvment most likely comes from the better representation of the input wind. Extrapolating this result, one may expect even better model results from further increasing resolution for the stormy extratropics, while the possibility of a further worsening in areas of low H_S cannot be excluded. Unfortunately, this hypothesis cannot be tested with the ERA winds, as ERA fields have a maximum effective horizontal resolution of $\approx 2°$ (see section 2.1), such that wave model resolutions higher than those of our HR model are meaningless.

3.3.3. Model error. Large peaks in H_S are directly related to local wind speed. Missing of wind speed maxima and consequently underestimation of wave height peaks are thus likely to result from too low a resolution of the wave model or the atmospheric model used to produce the winds. Resolution in both space and time has to be considered here. This view is confirmed by the results from the LR and the HR version, respectively, as explained above. The overestimation of low waves, however, cannot be explained by resolution effects.

Figure 5 shows the ratio of swell height to significant wave height. Comparison with Figure 2 shows that areas of overestimation of H_S coincide with areas of high swell-to-H_S ratio. It is thus tempting to speculate on the possibility that WAM produces too high swell. It has been suggested that the dissipation used in the propagation scheme is too low (P. Janssen, private communication, 1997).

Other explanations for the overestimation of waves in areas of light winds would be an overestimation of ERA winds in those areas or a poor calibration of WAM for these circumstances. However, erroneous swell propagation would also offer an explanation for the conflicting results from this study and those of *Romeiser* [1993] and *Janssen et al.* [1996]. While *Romeiser* [1993] also found an overestimation of low waves, *Janssen et al.* [1996] did not. However, the latter used a model with assimilation of altimeter wave heights (from ERS 1). As *Janssen et al.* [1996] noted, swell systems benefit most from assimilation, explaining the lack of overestimation of H_S. At the same time, assimilation might not have sufficient impact to influence the locally generated short-lived high waves, explaining the fact that the winter season scatter indices and biases found by *Janssen et al.* [1996] are comparable to those found here.

Clearly, the possibility of erroneous swell propagation needs more investigation.

3.3.4. Reanalysis error. If we tried to explain the mismatch in modeled and observed wave heights by errors in the ERA winds (thus implicitly assuming an error-free wave model), we would have to conclude that (mean) wind speeds are too low where wind speed is high (high latitudes) and too high in areas of low wind speeds. As discussed above, there is evidence for the first conclusion, with too low mean winds resulting from ERA missing wind peaks, which is a direct consequence of the spatial and temporal resolution chosen. The underestimation of high winds is, however, small. From Figures 1b and 2a the typical relative error of monthly mean H_S is found to be less than 10%, so that from (8) the relative error of monthly mean U_{10} is inferred to be less than 5%.

Evidence for the second conclusion could only be provided by further comparisons of ERA results with independent observations. This is beyond the scope of this paper. However, the above discusion shows that it might be possible to explain the overestimation of low waves by internal WAM errors.

3.3.5. Conclusion. From the foregoing discussion we conclude that the monthly mean ERA winds are slightly (less than 5%) too low in areas of high winds, while from this study it is not possible to draw a decisive conclusion on the quality of ERA winds at low wind speeds.

4. The Wave Climate

4.1. The Wave Climate 1979-1993

The prime objective of forcing the wave model with the ERA winds was to assess the quality of these winds. At the same time, however, the model output forms a 15-year global wave climatology that clearly has a value in its own right. Analyzing this climatology, one has to keep in mind the systematic errors discussed in the foregoing section and be careful when considering wave heights directly. However, changes in wave heights over time are more reliable. This can be inferred from the fact that trends derived from the LR and HR versions are largely identical. In the following, we only show results from the HR version.

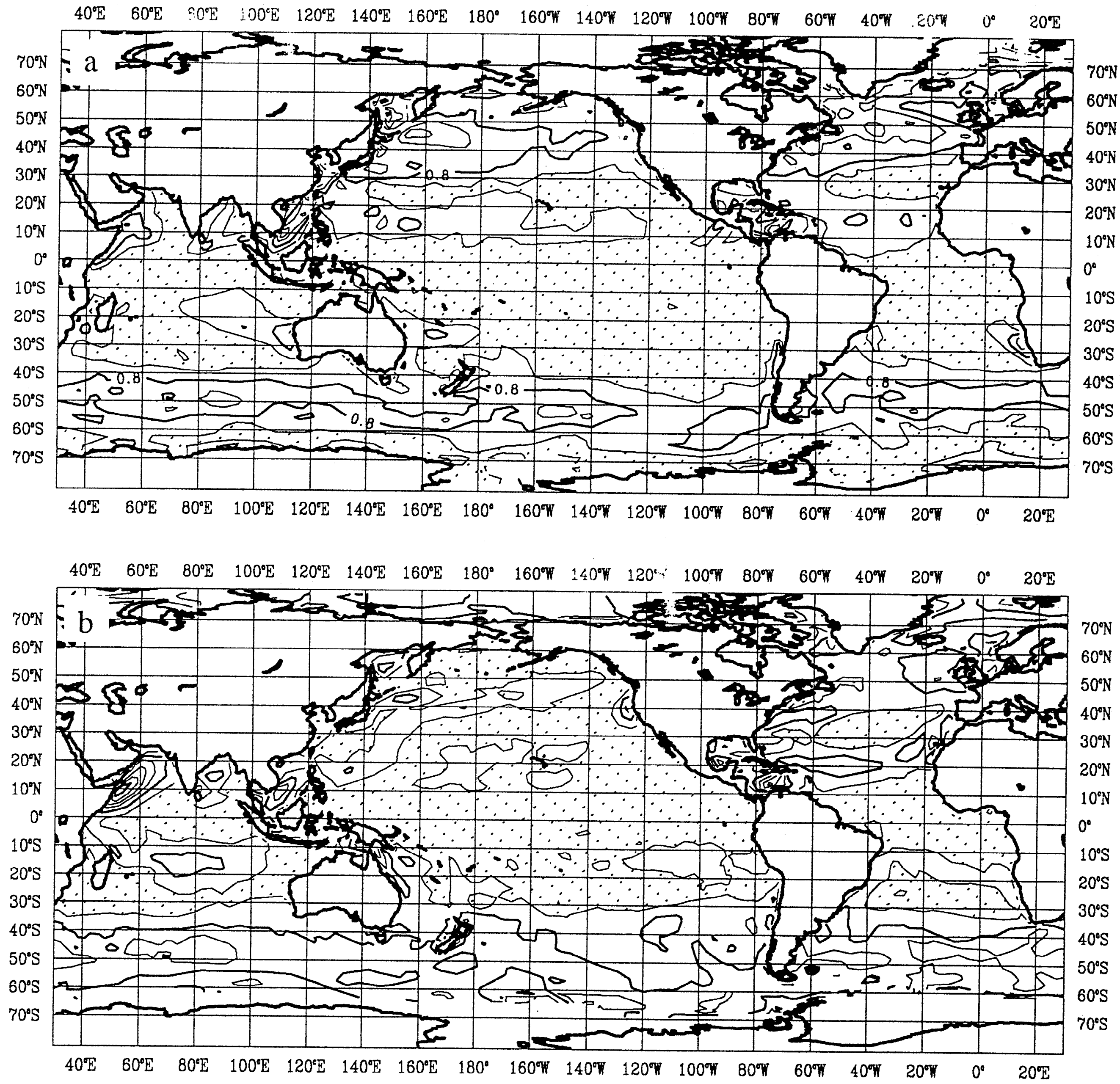

Figure 5. Ratio of swell height to significant wave height (HR model) for (a) January and (b) July 1988. Contour interval is 0.1 with stippling above 0.9.

Figure 6 shows the December-February and June-August means of H_S over the ERA period. As expected, the highest waves are found at the higher latitudes of the respective winter hemisphere. The waves in the SH are much higher than those in the NH and are lowest in the tropics. During winter, waves are higher in the North Atlantic than they are in the North Pacific. Along the coasts the largest seasonal mean wave heights are found in northwest Europe.

4.2. Trends in Wave Climate

For each calender month the linear trend of the monthly mean significant wave height has been calculated. In Figures 7a and 7b these trends are shown for the months January and July together with an indication of the areas where these trends are significant at the 95% level according to Student's t test. Not surprisingly, these trend patterns very much resemble those of U_{10} (not shown).

As can be seen, the largest trends occur on the respective winter hemispheres with maxima of more than 1.2 m/decade in the North Atlantic in January and 0.7 m/decade south of Africa in July. Together with an area in the southern tropical Pacific in July, these are also the only larger regions where the trends are significant during the two months. However, the trends vary very much from month to month.

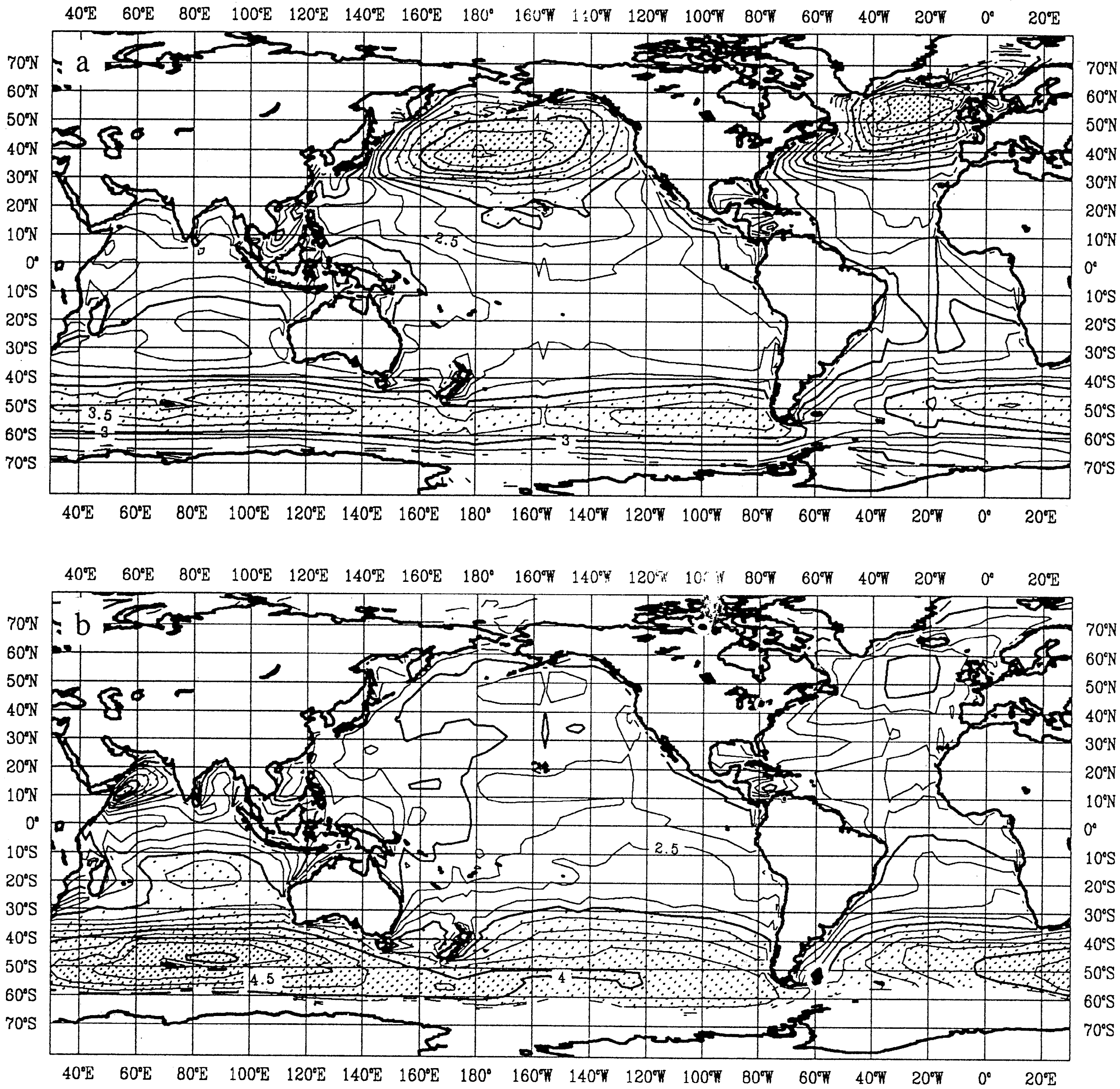

Figure 6. (a) DJF and (b) JJA average of H_S from the HR model. Contour interval is 0.25 m with stippling above 3 m. Every fourth line is thickened.

As an example, Figure 8 shows the trends in H_S and U_{10} for each calender month averaged over the North Atlantic (40°- 60°N and 10°- 40°W). At the 95% level, the H_S trends are significant only in April, September and October, and at the 90% level also in January. Therefore, the trend in significant wave height for the winter season (DJF) in this area (Figure 7c) reaches a maximum of only 0.4 m/decade, which furthermore is not significant. For the annual mean wave height (Figure 7d) in the North Atlantic the trend barely exceeds 0.1 m/decade and is significant only in the direct vicinity of Iceland. There is, however, a large area of significant negative trend of more than -0.15 m/decade along 30°N.

Kushnir et al. [1995] used a statistical method to hindcast North Atlantic winter (defined as November to March) wave heights over the period 1962-1986. Their trend pattern (their Figure 4a) very much resembles that found here (Figure 7c), but the amplitude is lower. This is probably because the statistical method that was used explains only part of the variance [*Kushnir et al.*, 1995].

Bacon and Carter [1991] found that annual mean significant wave heights over the North Atlantic increased by about 1 m over the 25-year period 1962-1986. These trends of $\approx$ 0.4 m/decade are much more than found here. However, care has to be taken as two different, only partially overlapping periods are considered. Obvi-

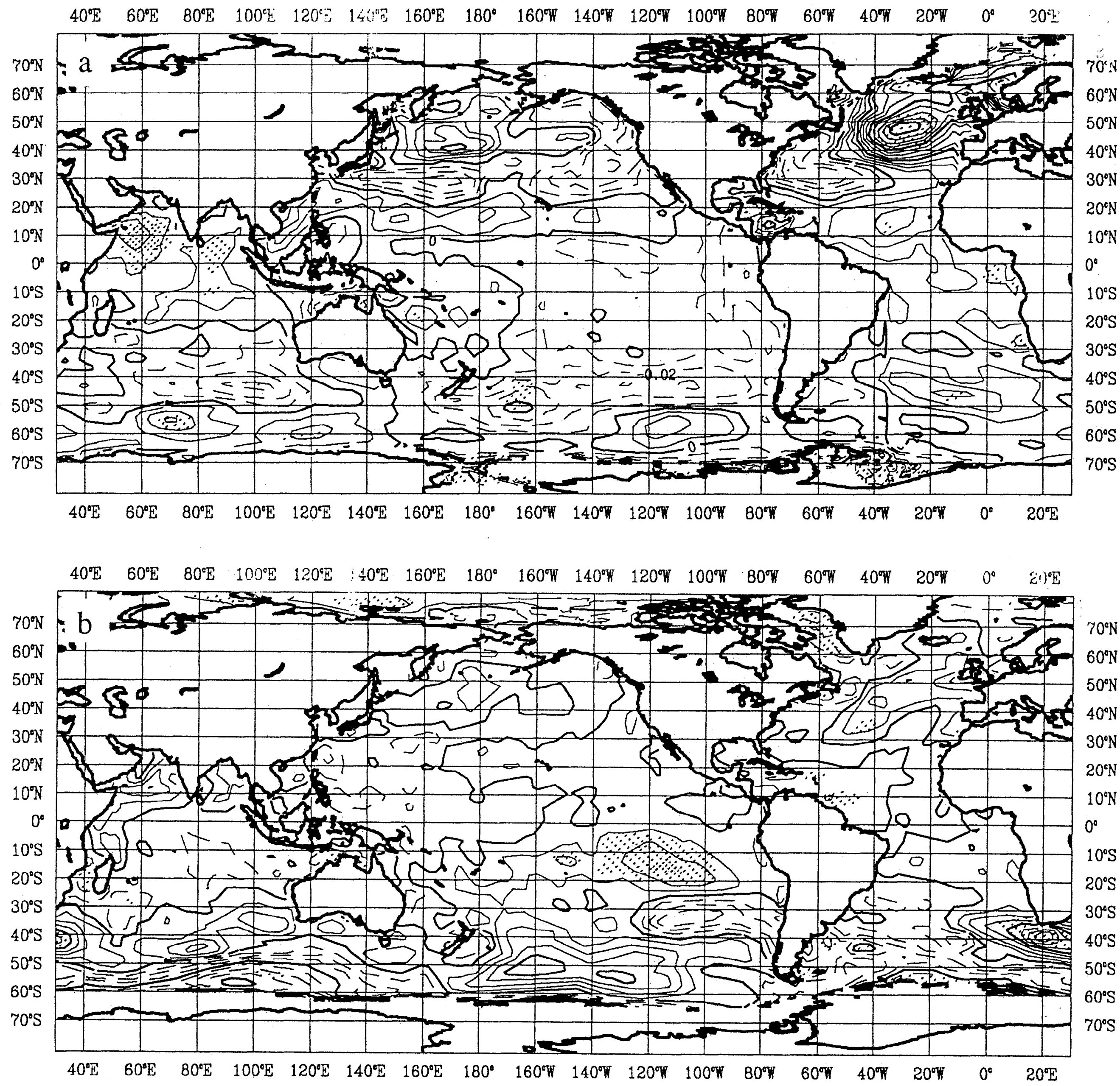

Figure 7. Linear trend of significant wave height (m/yr) over the ERA period for (a) January, (b) July, (c) DJF and (d) annual. In the stippled areas, these trends are significant at the 95% level according to Student's t test. Contour interval is 0.1 m/decade in Figures 7a-7c and 0.05 m/decade in Figure 7d. Negative isolines are dashed.

ously, the variability of North Atlantic climate is large, so that changes occurring over different periods need not be the same.

This can easily be seen by looking at the North Atlantic Oscillation (NAO), one dominant mode of variability over the North Atlantic [*Hurrell*, 1995]. It is described by the NAO index, the normalized pressure difference between Lisbon (Portugal) and Stykkisholmur (Iceland). Large values of the NAO index consequently indicate a larger-than-normal pressure difference between the Azores High and the Icelandic Low, resulting in larger wind speeds and hence higher waves. A statistical relationship between the NAO index and North Atlantic wave height was found by *Bacon and Carter* [1993].

From the time series given by *Hurrell* [1995] it can be seen that the NAO index increased from about -2 during 1960-1965 to about 1.5 in the first half of the 1980s and to about 2.5 during 1990-1995. Averaged out, the increase per year is thus much larger during

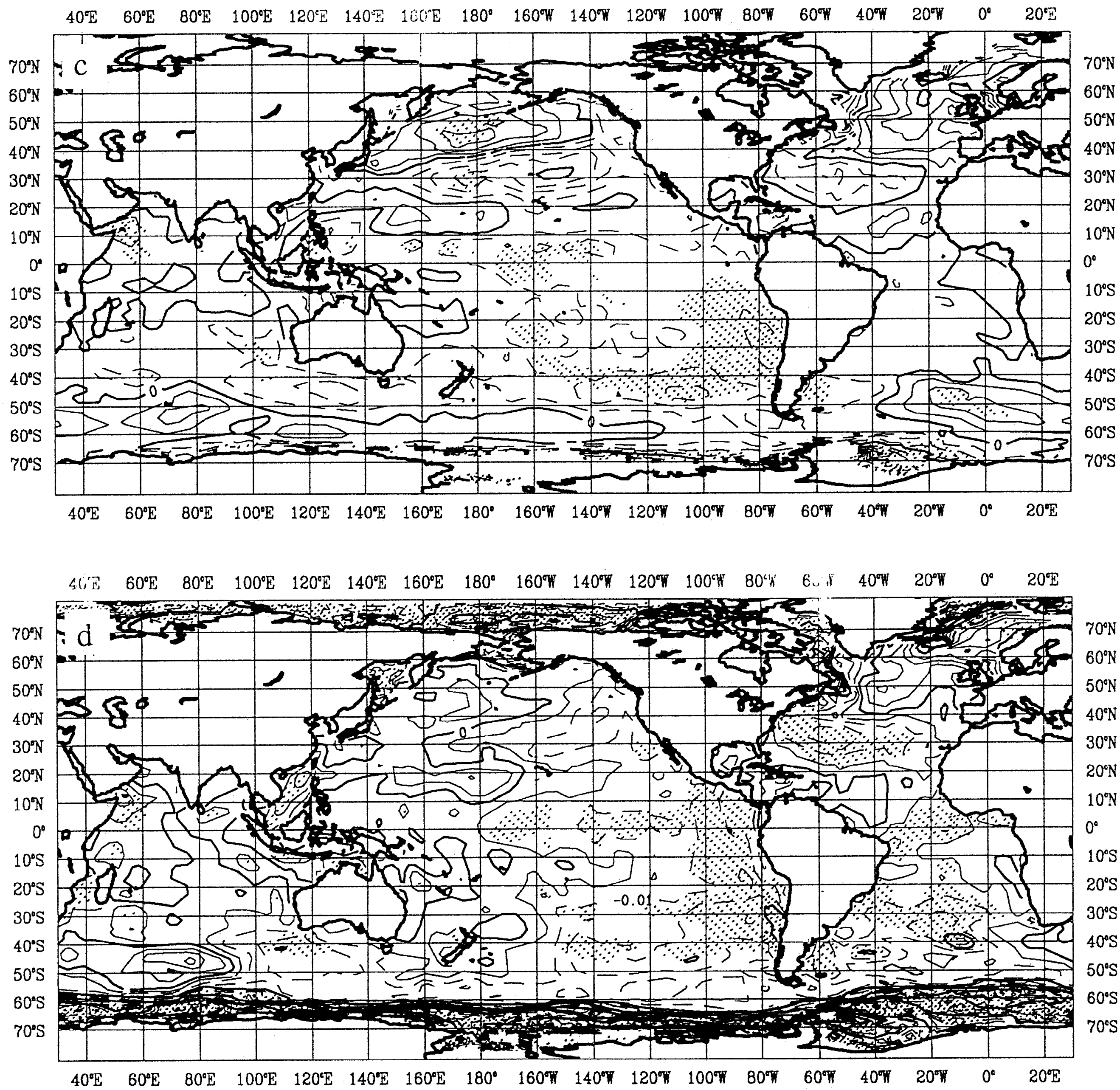

Figure 7. (continued)

the period considered by *Bacon and Carter* [1991] than during the ERA period. As the NAO index displays large variations on annual and decadal timescales, long-term trends can be deduced only from very long time series.

Besides looking at the wave heights themselves, one can also consider changes in wave statistics. To this end we computed the 10% and 90% exceedance wave heights and their trends for several regions (North Atlantic, 40°- 60°N and 10°- 40°W, North Pacific, 30°-60°N and 140°E - 120°W, and NH, SH, and tropics with latitudinal boundaries at 20°N and 20°S, respectively). These trends (not shown) form a similar picture as of those of H_S. Significant trends are found only for some months over the North Atlantic, while in the other regions the distribution of wave heights remained more or less the same over the ERA period. In the North Atlantic the 10% and 90% exceedance wave heights were seen to increase at a similar rate as H_S, the increase of which is thus accomplished by a shift of the whole wave height distribution toward higher waves.

5. Discussion and Conclusion

The ECMWF Reanalysis project (ERA) has produced a 15-year-long internally consistent description of the atmosphere. The surface winds from this data set have been used to drive two global versions of the WAM wave model, a low-resolution (LR, $3° \times 3°$) and a high-resolution (HR, $1.5° \times 1.5°$) one. The wave cli-

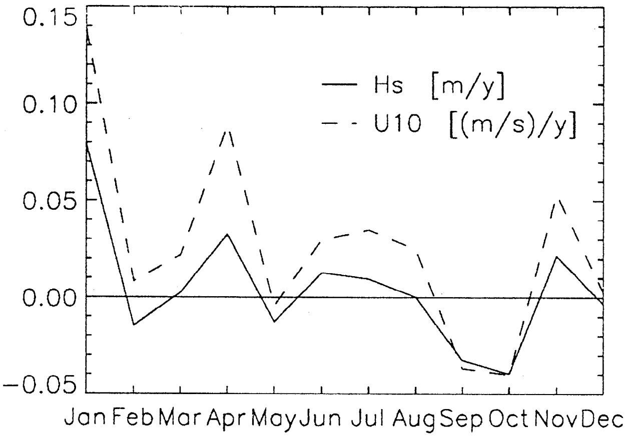

Figure 8. Linear trend of significant wave height (m/yr, solid line) and surface wind speed (ms^{-1}yr^{-1}, dashed) averaged over the North Atlantic (40°- 60°N and 10°- 40°W) as a function of calender month. Trends in H_S are significant at the 95% level in April, September and October. In January, the trend in both quantities is significant at the 90% level.

matologies from these runs have been analyzed focusing (1) on assessing the quality of the ERA surface winds by comparing modeled and observed wave heights, and (2) on changes in wave heights over the ERA period (1979 to 1993).

We have seen that the modeled wave heights are generally too low compared to satellite (altimeter) and buoy measurements in areas of high wind and waves, and too high elsewhere. Investigation of different possible reasons for this showed that the underestimation of high waves most probably is a resolution effect of both ERA and WAM, while the overestimation most probably results from internal WAM errors. Therefore, it is not possible to draw conclusions on the quality of ERA winds when the wind speed is low.

The HR version of WAM succeeded much better in capturing the high waves than the LR version, which thus proved inadequate to simulate global wave climate. Due to the finite resolution of the ERA wind fields (6 hours in time, effectively 2° in space) high winds can be missed, leading to an underestimation of high waves that significantly contribute to the mean wave heights at high latitudes. However, this underestimation is small. From our analysis we conclude that the monthly mean ERA winds are less than 5% too low in areas of high wind speeds, although for individual peaks underestimation is larger.

The analysis of trends in wave height over the ERA periods reveals that trend patterns vary much from month to month, and that trends are significant only in limited areas. Together, this indicates that the WAM output is unable to detect any significant change in wave climate during the ERA period.

Appendix: Technical Description of Wave Data Set

The WAM model was run in a low-resolution (LR) version on a 3° × 3° grid covering the whole globe between 72°N and 63°S, and a high-resolution (HR) version on a 1.5° × 1.5° grid covering the whole globe between 81°N and 81°S. The wave spectra of both versions are represented by 12 directions and 25 frequencies. The propagation time step is 1 hour for the LR version and 20 min for the HR version. Winds are updated every 6 hours (the synoptic hours of ERA) and held constant between updates. Unlike the LR version, the HR version takes sea ice into account by inhibiting waves at ice-covered grid points. A grid point is considered to be ice-covered if the surface temperature is below -1.75°C. However, this feature was erroneously switched off during the period 1979-1986. In this sense the results from the HR version are not homogeneous. Fortunately, the effects are confined to the vicinity of the ice margin.

Results from the LR version were saved every 12 hours (at 0000 and 1200 UTC), those from the HR version every 6 hours (at 0000, 0600, 1200, and 1800 UTC). Results from the HR version are stored in ECMWF's Mars archive using ECMWF local code table 2, version 140 for FM 92-VIII Ext. GRIB. Table A1 gives an overview of the quantities stored and the corresponding code numbers.

Due to some serious problems that were only discovered during the ERA production runs, the periods January 1979 to August 1980 and June 1990 to November 1992 had to be rerun [*Gibson et al.,* 1996]. The LR

Table A1. Quantities From the WAM Runs Stored in Mars

Code	Mars Abbreviation	Field	Units
229	SWH	significant wave height	m
230	MWD	mean wave direction	degrees
231	PP1D	peak period of 1d spectra	s
232	MWP	mean wave period	s
233	CDWW	coefficient of drag with waves	
234	SHWW	significant height of wind waves	m
237	SHPS	significant height of primary swell	m
238	MDPS	mean direction of primary swell	degrees
241	MU10	mean of 10 m wind speed	m/s
242	MDWI	mean wind direction	degrees
245[a]	WSTR[b]	wave-induced stress	

[a]This code figure is not from ECMWF local code table 2.
[b]According to (7).

version has also been rerun for these periods, but differences in H_S between the rerun and the original results proved to be small, not exceeding 10 cm for the monthly means. Therefore, the HR version has only been run for the original ERA version, labled EXPVER=01.

Acknowledgments. We would like to thank Peter Janssen and Jean Bidlot, without whose help with the WAM model this study would not have been possible. Thanks also to Hendrik Wallbrink and Hans Bonekamp for doing some of the analyses of the model results, and Peter Janssen, Sergej Gulev and Eva Bauer for fruitful discussions. ECMWF made this study possible by providing computer time. This work has been sponsored by the Dutch National Research Programme on Global Air Pollution and Climate Change under contract 951207.

References

Bacon, S., and D.J.T. Carter, Wave climate changes in the North Atlantic and North Sea, *Int. J. Climatol.*, 11, 545-558, 1991.

Bacon, S., and D.J.T. Carter, A connection between mean wave height and atmopheric pressure gradient in the North Atlantic, *Int. J. Climatol.*, 13, 423-436, 1993.

Cardone, V.J., H.C. Graber, R.E. Jensen, S. Hasselmann, and M.J. Caruso, In search of the true surface wind field in SWADE IOP-1: Ocean wave modelling perspective, *Global Atmos. Ocean Syst.*, 3, 107-150, 1995.

Carter, D.J.T., P.G. Challenor, and M.A. Srokosz, An assessment of Geosat wave height and wind speed measurements, *J. Geophys. Res.*, 97, 11,383-11,392, 1992.

Cotton, P.D., and D.J.T. Carter, Cross calibration of TOPEX, ERS-1, and Geosat wave heights, *J. Geophys. Res.*, 99, 25,025-25,033, 1994. (Correction, *J. Geophys. Res.*, 100, 7095, 1995.)

Gibson, R., P. Kållberg, and S. Uppala, The ECMWF Re-Analysis (ERA) Project, *ECMWF Newsl.*, 73, 7-17, 1996.

Graber, H.C., R.E. Jensen, and V.J. Cardone, Sensitivity of wave model predictions on spatial and temporal resolution of the wind field, paper presented at 4th International Workshop on Wave Hindcasting and Forecasting, Environment Canada, Banff, Alberta, Canada, Oct. 16-20, 1995.

Hurrell, J.W., Decadal trends in the North Atlantic Oscillation: Regional temperatures and precipitation, *Science*, 269, 676-679, 1995.

Janssen, P.A.E.M, G.J. Komen, and W.J.P. de Voogt, An operational coupled hybrid wave prediction model, *J. Geophys. Res.*, 89, 3635-3654, 1984.

Janssen, P.A.E.M., A.C.M. Beljaars, A. Simmons, and P. Viterbo, The determination of the surface stress in an atmospheric model, *Mon. Weather Rev.*, 120, 2977-2985, 1992.

Janssen, P.A.E.M., B.J. Hansen, and J. Bidlot, Verification of the ECMWF wave forecasting system against buoy and altimeter data, *ECMWF Tech. Memo. 229*, Eur. Cent. for Medium-Range Weather Forecasts, Reading, England, 1996.

Komen, G.J., L. Cavaleri, M. Donelan, K. Hasselmann, S. Hasselmann, and P.A.E.M. Janssen, Dynamics and Modelling of Ocean Waves, 532 pp., Cambridge Univ. Press, New York, 1994.

Kushnir, Y., V.J. Cardone, J.G. Greenwood, and M.A. Cane (1995), Link between North Atlantic climate variability of surface wave height and sea level pressure, paper presented at 4th International Workshop on Wave Hindcasting and Forecasting, Environment Canada, Banff, Alberta, Canada, Oct. 16-20, 1995.

Romeiser, R., Global validation of the wave model WAM over a one-year period using Geosat wave height data, *J. Geophys. Res.*, 98, 4713-4726, 1993.

Sanders, J.W., A growth-stage scaling model for the wind-driven sea, *Dtsch. Hydrogr. Z.*, 29, 136-161, 1976.

Stockdale, T., ERA surface fluxes: early impressions, in *Air-Sea Flux Fields for Forcing Ocean Models and Validating GCMs, Proceedings of a WCRP workshop held at Reading, UK, 24-27 October 1995, Rep. WMO/TD 762*, World Meteorol. Organ., Geneva, 1996.

WAMDI Group, The WAM model - A third generation ocean wave prediction model. *J. Phys. Oceanogr.*, 18, 1775-1810, 1988.

Zambresky, L., A verification study of the global WAM model. December 1987 - November 1988, *ECMWF Tech. Rep. 63*, Eur. Cent. for Medium-Range Weather Forecasts, Reading, England, 1989.

P.D. Cotton, Southampton Oceanography Centre, James Rennell Division, Southampton SO14 3ZH, England, UK. (e-mail: Dave.Cotton@soc.soton.ac.uk)

A. Komen and A. Sterl, Koninklijk Nederlands Meteorologisch Instituut, Postbus 201, NL-3730 AE De Bilt, Netherlands. (e-mail: sterl@knmi.nl)

(Received March 25, 1997; revised September 12, 1997; accepted November 3, 1997.)